Now the two frequency offset values are suitably modified as

$$\left.\begin{aligned}\Delta f_1 &= -f_r \frac{0.4185}{2}\frac{ds}{s}\\ \Delta f_2 &= f_r 0.4185\frac{ds}{s}\end{aligned}\right\} \quad \text{for } \varepsilon_r < 4.5$$

and

$$\left.\begin{aligned}\Delta f_1 &= -f_r 0.4185\frac{ds}{s}\\ \Delta f_2 &= f_r \frac{0.4185}{2}\frac{ds}{s}\end{aligned}\right\} \quad \text{for } \varepsilon_r \geq 4.5$$

The resonant frequencies corresponding to ports 1 and 2, respectively, are given by

$$f_1 = f_r + \Delta f_1 \tag{2}$$

$$f_2 = f_r + \Delta f_2 \tag{3}$$

where $c$ is the velocity of light in free space, $s = \pi r^2$ (area of the original circle) and $(s - \Delta s)$ is the overlapping area of the two circles. The theoretical resonant frequencies for ports 1 and 2 are 2.609 and 3.129GHz, respectively. The experiment has been repeated with substrates of different thickness and dielectric constant. The agreement between theoretical and experimental resonance frequencies is found to be good, except for a slight error that could be due to tolerances in dielectric constant, fabrication etc. Generally, the above analysis can predict the resonant frequencies with an error of less than 5%.

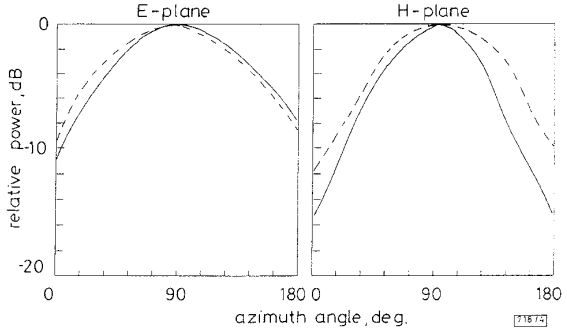


**Fig. 4** *E-plane and H-plane radiation patterns of the antenna at the centre frequencies of the two ports*

——— port 1
– – – – port 2

*Conclusion:* A novel dual port broad-band microstrip antenna resonating at two frequencies and providing orthogonal polarisations with very good isolation between the two ports is reported. The gain of the antenna is comparable to that of a standard circular patch microstrip antenna. This antenna may find application in systems where dual frequency operation with large bandwidth is required.

*Acknowledgment:* The authors acknowledge the University Grants Commission (UGC), Government of India for providing financial assistance.


*19 June 1996*
*Electronics Letters Online No: 19961056*

M. Deepukumar, J. George, C.K. Aanandan, P. Mohanan and K.G. Nair (*Department of Electronics, Cochin University of Science and Technology, Cochin 682 022, India*)

## References

1 IWASAKI, H.: 'Proximity coupled linearly polarised patch antenna for dual frequency use', *Electron. Lett.*, 1995, **31**, (15), pp. 1212–1213

2 SALVADOR, C., BORSELLI, L., FALCIANI, A., and MACI, S.: 'Dual frequency planar antenna at S and X bands', *Electron. Lett.*, 1995, **31**, (20), pp. 1706–1707

3 BAHL, I.J., and BHARTIA, P.: 'Microstrip antennas' (Artech House, Dedham, MA, 1981)

4 JAMES, J.R., and HALL, P.S.: 'Handbook of microstrip antennas' (Peter Peregrinus Ltd, IEE Engineers IV series, 1989)

# Programmable dispersion matrix using Bragg fibre grating for optically controlled phased array antennas

D.T.K. Tong and M.C. Wu

*Indexing terms: Gratings in fibres, Optical control of microwaves*

A programmable dispersion matrix implemented with Bragg fibre gratings is demonstrated in conjunction with a multiwavelength laser source for use in optically controlled phased array antennas. Relative time delays are experimentally measured using a prototype programmable dispersion matrix with 2 bit resolution and the results agree well with the theoretical prediction.

*Introduction:* In addition to the obvious advantages of optical fibres, they can be used to produce optically controlled phased array antennas (OCPAAs) with true time delay features, large instantaneous bandwidth and squint-free operation. Recently, there has been increasing interest in exploiting the wavelength domain of lightwaves to reduce the overall system complexity and cost [1 – 7]. For example, we have previously reported a hardware-compressive multiwavelength OCPAA (MWOCPAA) system using a programmable dispersion matrix (PDM) in conjunction with a multiwavelength laser source [7]. In such scheme, an 'optical wavelength-to-array element' correspondence is established. The PDM is implemented with dispersive fibre to generate relative time delay among the optical wavelengths and hence control the beam angle. One drawback of this approach is that long fibres (~kilometres) are required to create large time delays, and therefore system size becomes an issue. Moreover, the dispersion-generated time delay is accompanied by dispersion-induced signal distortion. To ease these problems, we demonstrate in this Letter a PDM implemented using a Bragg fibre grating as a 'tailorable dispersive' element.

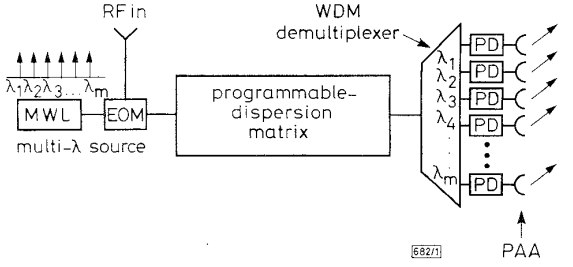


**Fig. 1** *Schematic diagram of MWOCPAA using a multiwavelength laser source and a PDM*

*Principle:* Fig. 1 illustrates the schematic diagram of the MWOCPAA. The multiwavelength laser source provides optical wavelengths $\{\lambda_1, \lambda_2, ..., \lambda_m\}$. A microwave signal is modulated onto all the optical wavelengths simultaneously by an external electro-optic (EO) modulator. The modulated lightwaves are then sent through the PDM for true-time delay processing. The details of the PDM are shown in Fig. 2. In general, a PDM with $n$-bit resolution consists of $n$ dispersive elements and $(n+1)$ $2 \times 2$ optical

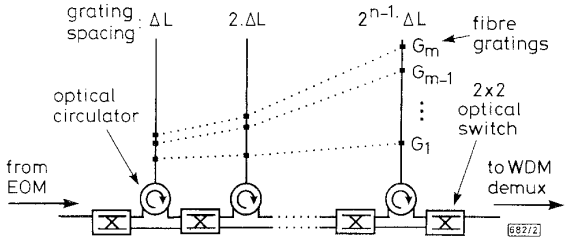


**Fig. 2** *n-bit resolution PDM implemented with fibre gratings*

switches. The dispersive elements in this demonstration are realised by Bragg fibre gratings. A series of grating reflectors are fabricated at different positions along the fibre. Each grating is

matched to a different wavelength from the multiwavelength source and therefore $G_i$ reflects $\lambda_i$. The spacings between the gratings are arranged so that the relative time delay between adjacent optical wavelengths exhibited at each stage increases exponentially, i.e. $\tau_1$>, $2\cdot\tau_1$, $2^2\cdot\tau_1$, ..., $2^{n-1}\cdot\tau_1$. Here, $\tau_1$ is the relative time delay in the first stage of the PDM:

$$\tau_1 = \frac{2 \cdot \Delta L_1 \cdot n}{c} \quad (1)$$

where $\Delta L_1$ is the grating spacing in the first stage, $n$ is the refractive index of the fibre, and $c$ is the velocity of light in free space. An optical circulator is used to route the lightwaves. By programming the $2 \times 2$ optical switches, the total relative time delay generated by the PDM, $\tau_{PDM}$, can vary from 0 to $(2^n-1)\cdot\tau_1$ in increments of $\tau_1$. At the receiver, a wavelength-division-multiplexed (WDM) demultiplexer routes $\lambda_i$ to the $i$th element of the array, giving rise to linear time shifts of $\{0, \tau_{PDM}, 2\cdot\tau_{PDM}, ..., (m-1)\cdot\tau_{PDM}\}$ across the array elements. The steering angle $\theta$ is

$$\theta = \sin^{-1}\left(\frac{c \cdot \tau_{PDM}}{\Lambda}\right) \quad (2)$$

for all RF frequencies, where $\Lambda$ is the distance between array elements.

*Experiment:* To demonstrate the concept of PDM, an experimental prototype with 2bit resolution was constructed. An 80GHz monolithic passive CPM InGaAs-InGaAsP quantum well laser was used as the multiwavelength source [7]. The reduced mode partition noise in the mode-locked laser makes it a suitable multiwavelength source for this application [8]. Four gratings were implemented at each stage of the PDM to reflect optical wavelengths at 1546.85, 1547.47, 1548.09 and 1548.71nm from the CPM laser. The grating spacings in the first and second stages of the PDM were 1 and 2cm, respectively. All the gratings used in the setup had a reflectivity of 85% and an FWHM reflection band of 0.15nm. The RF signal was applied to all wavelengths through an external EO modulator with 5GHz bandwidth. A tunable fibre Fabry-Perot filter with 10GHz bandwidth was placed after the PDM to select different wavelength channels for time delay measurement. The selected channel was fed to a high speed photodetector. The time delay was measured using an HP 8510 microwave network analyser.

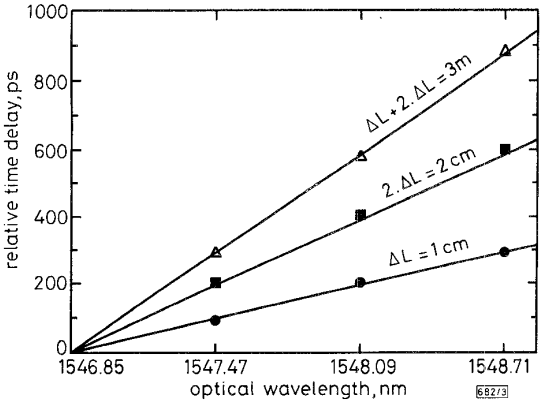


**Fig. 3** *Relative time delay at various optical wavelengths generated by fibre grating in first stage ($\Delta L$), second stage ($2\cdot\Delta L$) and both stages of PDM ($\Delta L+2\cdot\Delta L$)*

The lines represent the theoretical prediction and markers the measured data

*Results:* Fig. 3 shows the measured relative time delay as a flinction of optical wavelength. The time delays were measured relative to that at $\lambda$ = 1546.85nm. Using either grating or both simultaneously, the measured time delays between adjacent wavelength obtained from these measurements were 98.38, 201.30 and 292.59ps, compared to the theoretical values of 97.33, 194.67 and 292ps, respectively. These small differences are due to deviations in grating positions and mismatches between optical wavelengths and grating pitches.

*Summary:* In conclusion, we have demonstrated a programmable dispersion matrix using a grating fibre for applications such as OCPAAs. Compared to a PDM comprising dispersive fibre, the use of a fibre grating in a PDM as a tailorable dispersive element significantly reduces the system size and eliminates dispersion-induced signal distortion.

*Acknowledgment:* The authors would like to thank J.C. Brock of TRW for providing the optical circulator used in this experiment. This work is supported by ARPA NCIPT and the Parkard Foundation.


*1 July 1996*
*Electronics Letters Online No: 19961042*

D.T.K. Tong and M.C. Wu (*UCLA, Electrical Engineering Department, 405 Hilgard Avenue, Los Angeles, CA 90095-1594, USA*)

**References**

1 GOUTZOULIS, A., and DAVIES, K.: 'All-optical hardware compressive wavelength-multiplexed fibre optic architecture for true time delay steering of 2-D phased array antennas', *Proc. SPIE*, 1992, **1703**, pp. 604–614
2 SOREF, R.: 'Optical dispersion technique for time-delay beam steering', *Appl. Opt.*, 1992, **31**, pp. 7395–7397
3 ESMAN, R.D., FRANKEL, M.Y., DEXTER, J.L., GOLDBERG, L., PARENT, M.G., STILWELL, D., and COOPER, D.G.: 'Fiber-optic prism true time-delay antenna feed', *IEEE Photonics Technol. Lett.*, 1993, **5**, pp. 1347–1349
4 FREITAG, P.M., and FORREST, S.R.: 'A coherent optically controlled phased array antenna system', *IEEE Microw. Guid. Wave Lett.*, 1993, **3**, pp. 293–295
5 LEMBO, L.J., HOLCOMB, T., WICKHAM, M., WISSEMAN, P., and BROCK, J.C.: 'Low-loss fibre optic time-delay element for phased-array antennas', *Proc. SPIE*, 1994, **2155**, pp. 13–23
6 FETTERMAN, H.R., CHANG, Y., LEVI, A.A., COHEN, D., and NEWBERG, I.L.: 'Serially fed optically controlled phased arrays'. SPIE Annual Meeting 1996, 7–8 August 1996, Denver, Colorado, USA, Paper 2844–33
7 TONG, D.T.K., and WU, M.C.: 'A novel multiwavelength optically controlled phased array antenna with a programmable dispersion matrix', *IEEE Photonics Technol. Lett.*, 1996, **8**, pp. 812–814
8 HO, P.T.: 'Phase and amplitude fluctuations in a mode-locked laser', *IEEE J. Quantum Electron.*, 1985, **QE-21**, pp. 1806–1813

## Low dissipation power and high linearity PCS power amplifier with adaptive gate bias control circuit

K.-J. Youn, B. Kim, C.-S. Lee, S.-J. Maeng, J.-J. Lee, K.-E. Pyun and H.-M. Park

*Indexing terms: Linearisation techniques, Radiofrequency amplifiers*

A new PCS power amplifier with gate bias control circuit has been developed for high efficiency at low output power level, and for high linearity at high output power level. The efficiency at an average operating power of 16dBm was improved to 10.5%, and the $IMD_3$ at the maximum operating power of 27dBm to –33dBc.

*Introduction:* Power amplifiers with high power-added efficiency (PAE) and low intermodulation distortion have been required in CDMA personal communications service (PCS) systems to reduce power consumption and bit error rate. There were many reports on improving efficiency and linearising output power by methods such as feedforward [1] and predistortion [2]. However, because most of the efforts were focused on improving maximum efficiency near saturation output power, the efficiencies at the average operating power were poor. Moreover, most of the linearising techniques are difficult to apply to small size amplifiers for hand held phones due to their complexity. Meanwhile, there were some reports on improving efficiency [3] and intermodulation distortion [4] by adjusting gate bias controlled by input signal level. But, to our knowledge, there were no reports on achieving high efficiency and low third-order intermodulation distortion ($IMD_3$), simultaneously.